Optical dispersion relations for crystalline and microcrystalline silicon

H. Touir* and P. Roca i Cabarrocas
Laboratoire de Physique des Interfaces et des Couches Minces (UMR 7647 CNRS), Ecole Polytechnique, 91 128 Palaiseau, Cedex, France

(Received 2 August 2001; revised manuscript received 26 November 2001; published 11 April 2002)

A different method is presented to model the optical functions of crystalline and microcrystalline semiconductors. This model incorporates the full electronic band structure and the lifetime broadening, and is applicable at the energies below and above the lowest gap. With the examples of crystalline and microcrystalline silicon, we demonstrate the good agreement between the simulation and the optical spectra (i.e., dielectric function) and both the realistic electronic band structure and the realistic lifetime broadening. It is shown that the general change in the optical functions in microcrystalline silicon materials compared to their homologue crystalline materials is due to the effects of the limited crystallite size and of the medium structural disorder (i.e., ''random'' distribution of the texture—size, shape, and crystallographic orientation—of crystallites), which yields to the change in shape of the electronic conduction bands and the decrease of the lifetime of the excited states.

DOI: 10.1103/PhysRevB.65.155330 PACS number(s): 71.20.Nr, 71.23.−k, 78.66.Li

I. INTRODUCTION

The interpretation of the optical measurements on crystalline and microcrystalline semiconductors, at the energies below and above the lowest gap, requires a detailed knowledge of both the electronic band structure and the wave functions in relation with the intrinsic structural properties. For crystalline semiconductors, where the electronic states are described with the well-known Bloch functions, there are many sophisticated methods for calculating the electronic band structures.[1] As for the case of microcrystalline semiconductors, where the translation periodicity of the lattice is broken and therefore the electronic wave functions are not described by simple Bloch functions, the calculation of the electronic band structure and the wave functions require more sophisticated methods.[2,3] These methods are not only complicated but also are not adequate for the parametrization of the optical functions of crystalline and microcrystalline semiconductors. These parametrizations are indeed useful to interpret the optical functions of thin films. This is particularly true in the case of the spectroscopic ellipsometry measurements, where one measures the functions of the Fresnel coefficients, which then must be related to the film parameters such as thickness, surface roughness, and dielectric function.

The fundamental electronic excitation spectrum of a substance is generally described in terms of the energy-dependent complex electronic dielectric function $\varepsilon(E)$. Either the real part $\varepsilon_1(E)$ or the imaginary part $\varepsilon_2(E)$ contain all the desired response information, since causality arguments relate $\varepsilon_1(E)$ and $\varepsilon_2(E)$ via the well-known Kramers-Kronig relation:

$$\varepsilon_1(E)=1+\frac{2}{\pi}P\int_0^{+\infty}\frac{E'\varepsilon_2(E')}{E'^2-E^2}dE',$$
$$\varepsilon_2(E)=-\frac{2}{\pi}P\int_0^{+\infty}\frac{E'(\varepsilon_1(E')-1)}{E'^2-E^2}dE', \quad (1)$$

where P denotes the principal part of the integral.

During the last few years microcrystalline silicon (μc-Si) films have appeared as a promising material for thin-films devices such as solar cells, sensors, and thin-film transistors. At present the optical characterization of the films, which depends strongly on the preparation conditions, has been the subject of the considerable studies, but the interpretation of the optical data is highly debated.[4–6] In the visible and the near-infrared regions the optical edge of μc-Si films is increased compared to crystalline silicon (c-Si).[4–7] This behavior has been attributed either to the absorption by the amorphous fraction (noncrystallized) supposed very important in the material[5,6] or by the stress effect in the microcrystalline network.[6] However, these hypotheses do not completely explain the optical edge in μc-Si materials and have been challenged by the effect of the structural disorder at the medium range (due to the variation of the texture—size, shape, and crystallographic orientation—of crystallites).[7] As for in the ultraviolet and the visible regions either the real part (ε_1) or the imaginary part (ε_2) of the dielectric function $\varepsilon(E)$ of μc-Si materials are considerably different from those of c-Si.[8] The typical spectrum of the imaginary part of the dielectric function for μc-Si materials is characterized by (i) a marked decrease in the intensity, (ii) greatly weakened 3.4-eV (E_1), 4.2-eV (E_2), and 5.4-eV (E'_1) structures, and (iii) a pronounced tail below the c-Si fundamental-absorption threshold, which depend strongly on the preparation conditions. In order to interpret this behavior, μc-Si layers have been modeled using the Burggeman effective-medium approximation, consisting of a mixture of crystalline silicon, amorphous silicon, and voids.[8–10] It is worth noticing that the modeling using the effective-medium theory can be also achieved by polycrystalline silicon (p-Si) with large or fine grains. Nevertheless, this method does not fit very well the dielectric function and therefore does not provide the information about film parameters (i.e., thickness, surface roughness, and dielectric function).[9,10] This is particularly true for μc-Si layers with small crystallite size, where their optical response is considerably different from those of c-Si and p-Si.[9,10] It is also common practice to simulate the opti-

cal functions of semiconductors with a dispersion formula.[11–14] These models approximate the interband transitions between the band states over all vectors in the Brillouin zone (BZ) with the optical response at the critical-point structure of the electronic density of states, and do not incorporate the full band structure in the Brillouin zone.

In this paper we present a different model for the parametrization of the optical functions of crystalline and microcrystalline semiconductors at the energies below and above the lowest gap. This model incorporates the full electronic band structure and the lifetime broadening and its parameters are physically significant. With the examples of *c*-Si and μc-Si, we shall demonstrate the good agreement between the simulation and the optical spectra (i.e., dielectric function) and both the realistic electronic band structure and the realistic lifetime broadening. We shall show that the general change in the optical functions in a microcrystalline material compared to their homologue crystalline material is due to the effects of the limited crystallite size and of the medium structural disorder (i.e., ''random'' distribution of the texture—size, shape, and crystallographic orientation—of crystallites), which yields to the change in shape of the conduction bands and the decrease of the lifetime of the excited states.

II. MODEL

In perfect crystalline semiconductors, the imaginary part of the dielectric function $\varepsilon_2(E)$ is given within the first-order perturbation theory of the radiation field effect on the crystal electronic states, by[15]

$$\varepsilon_2(E)=4\pi^2e^2\int_{\mathrm{BZ}}\frac{2V}{(2\pi)^3}|R_{cv}(k)|^2 \times\delta[E_C(k)-E_V(k)-E]d^3K, \tag{2}$$

where V is the crystal volume [$2V/(2\pi)^3$ being the density of allowed **k** vectors in the BZ], e is the electron change, E is the photon energy, E_c (E_v) is the energy of the conduction (valence) state, R_{cv} is given by $R_{cv}=\langle C|nR|V\rangle$, where **n** is the polarization vector of the incident light, **R** is the position operator, $|V\rangle$ ($|C\rangle$) is the wave function of the valence (conduction) band state. In Eq. (2) the integral is over all **k** vectors in the Brillouin zone (BZ). As stressed above, the sophisticated calculation of $\varepsilon_2(E)$ cannot allow the parametrization of the optical functions. The sophisticated calculation of the integral (2) is indeed performed numerically by sampling the Brillouin zone, which has generally a very complicated shape, and computing the energy levels of the valence and the conduction bands at every **k** point. In the next sections, we shall provide a number of simplifying approximations of Eq. (2), which allow the parametrization of the optical functions of crystalline materials as well as microcrystalline materials.

A. Pseudoisotrope approximation

To simplify the calculation of Eq. (2), we have approximated the Brillouin zone by the concentric spheres, where the center and the radius are equal to the center of the Brillouin zone and Brillouin-zone boundaries in the high symmetries, respectively. Then, we have assumed that in each sphere the electronic bands structures are isotrope. Using these approximations, which we call pseudoisotrope approximations, as well as spherical coordinates, we have transformed Eq. (2) into

$$\varepsilon_2(E)=4\pi^2e^2\sum_i\sum_j\int_{j\mathrm{BZ}}\frac{2V}{(2\pi)^3}|R_{ijcv}(k)|^2 \times\delta[E_{ijc}(k)-E_{ijv}(k)-E]4\pi k^2dk, \tag{3}$$

where the sum i and j refer to over all pair of bands and to the axis number of the high symmetries in the Brillouin zone, respectively. It is important to notice that our pseudoisotrope approximation not only allows the simplification of the computation of the optical functions but also allows the calculation with a large number of points at every **k**, which improves the accuracy of the results. It is well known indeed that the result accuracy of the numerical computation of the optical functions depends strongly on the number of points in **k** space.[16]

B. Damping effect

It is well known that the optical transitions are strongly affected by the damping effect due either to the collective vibration of atoms (i.e., phonons), due to the thermal agitation, or to the structural defects of the crystalline network which decrease the lifetime of the photocreated carriers. The broadening parameter can be expressed by a sum of two different contributions: $\Gamma(T)=\Gamma_0+\Gamma_{\in}(T)$, where Γ_0 is independent of the temperature, arising mainly from the lattice defects, and $\Gamma_{\in}(T)$ is a contribution through the emission and the absorption of the phonons of the average energy $\in$, proportional to $[\exp(\in_{/KT})]^{-1}$. This lifetime broadening effect can be easily introduced in a phenomenological manner in Eq. (3) by replacing the Dirac function by the Lorentzian function, as

$$\varepsilon_2(E)=4\pi^2e^2\sum_i\sum_j\int_{j\mathrm{BZ}}\frac{2V}{(2\pi)^3}|R_{ijcv}(k)|^2 \times\frac{1}{\pi}\frac{\Gamma_{ij}4\pi k^2dk}{[E_{ijc}(k)-E_{ijv}(k)-E]^2+\Gamma_{ij}^2}, \tag{4}$$

where Γ_{ij} is the linewidth of the Lorentzian function, which can be linked to the lifetime τ_{ij} of the excited state $|C\rangle$ via the Heisenberg principle: $\Gamma_{ij}\cong\hbar/2\tau_{ij}$. It is worth noticing that from a theoretical point of view, the lifeime broadening for each conduction band depends on the **k** vector in the BZ.[2,3] For simplicity we have assumed that the lifetime broadenings are constant for each conduction band.

C. Optical matrix elements approximation

In this section we develop an analytic expression of the optical matrix elements. To obtain the analytic expression of

the optical matrix elements R_{ijcv} as a function of the electronic band structure we multiply Eq. (4) by the energy and we integrate

$$\int E\varepsilon_2(E)dE \cong 4\pi^2 e^2 \sum_i \sum_j \int_{jBZ} \frac{2V}{(2\pi)^3} \times [E_{ijc}(k) - E_{ijv}(k)] |R_{ijcv}(k)|^2 4\pi k^2 dk. \tag{5}$$

Here, we have used the approximation

$$\int \frac{1}{\pi} \frac{\Gamma}{(x-x_0)^2 - \Gamma^2} f(x) \cong f(x_0).$$

Then, we use the oscillator strength f_{ijvc}

$$f_{ijvc}(k) = \frac{2m[E_{ijc}(k) - E_{ijv}(k)] |R_{ijcv}(k)|^2}{\hbar^2}, \tag{6}$$

and its sum rule,

$$\sum_i \sum_j \int_{jBZ} \frac{2V}{(2\pi 2)^3} f_{ijc}(k) 4\pi k^2 dk = N_{\text{eff}}, \tag{7}$$

where N_{eff} is the effective density of the valence electrons.

Assuming that the oscillator strength varies slowly with **k** vectors for a pair of bands and their magnitude is approximated by N/n [where N is the orbital number in each energy band and n is the pair number of the bands intervening to $\varepsilon_2(E)$], the oscillator strength becomes

$$f_{ijcv}(k) = \frac{N}{n} = \frac{1}{V_{\text{BZ}}} \frac{N_{\text{eff}}}{n} \frac{(2\pi)^3}{2V}, \tag{8}$$

where V_{BZ} is the sum volume of the concentric spheres in the Brillouin zone.

Thus, from Eq. (6) and (8), the matrix elements for a pair of bands become

$$|R_{ijcv}(k)|^2 = \frac{1}{V_{\text{BZ}}} \frac{N_{\text{eff}}}{n} \frac{(2\pi)^3}{2V} \frac{\hbar^2}{2m[E_{ijc}(k) - E_{ijv}(k)]}. \tag{9}$$

This equation shows that the optical matrix elements R_{ijcv} and therefore the optical transition probability is proportional to the inverse of the energy difference $(E_{ijc} - E_{ijv})$ between the conduction and the valence bands. This behavior shows that the higher $(E_{ijc} - E_{ijv})$ is, the smaller the transition probability, as it should be because when the value of $(E_{ijc} - E_{ijv})$ tends to infinity the transition probability tends to zero. It is worth noticing that the assumption about the variation of the oscillator strength for a pair of bands is associated with a single optical transition as the classical Lorentz dispersion formula for an assembly of weakly photocreated carriers. It is also important to notice that as a consequence of the sum rule of the oscillator strength and the optical matrix elements approximation, the sum rule of $\varepsilon_2(E)$ is taken into account:

$$\int E\varepsilon_2(E)dE = \frac{\pi}{2} E_p^2, \tag{10}$$

where $E_p [E_p = (\hbar^2 4\pi N_{\text{eff}} e^2/m)^{1/2}]$ is the plasma energy. This sum rule is indeed often used to test the consistency of the approximations involved in phenomenological optical models. Taking into account the analytic expression of the optical matrix elements [i.e., Eq. (9)], the imaginary part $\varepsilon_2(E)$ of crystalline semiconductors can be expressed as

$$\varepsilon_2(E) = \frac{\pi}{2} E_p^2 \frac{1}{V_{\text{BZ}}} \sum_i \frac{1}{n} \sum_j \int_{jBZ} \frac{1}{E_{ijc}(k) - E_{ijv}(k)} \times \frac{1}{\pi} \frac{\Gamma_{ij} 4\pi k^2 dk}{(E_{ijc}(k) - E_{ijv}(k) - E)^2 + (\Gamma_{ij})^2} \tag{11}$$

with

$$E_{ijc}(k) = \sum_{n=0}^{4} c_{ij2n} k^{2n}, \quad E_{ijv}(k) = \sum_{n=0}^{4} v_{ij2n} k^{2n}.$$

Here, the valence and conduction bands are approximated by polynomials. The choice of the even polynomial is dictated by the numerical approximation of the integral over the BZ_j, where the bands are supposed isotropes.

D. Effect of limited crystallite size and structural disorder

In the case of a microcrystalline semiconductor, the optical functions are strongly different from their homologue crystalline. Nevertheless, these changes keep the main characteristics. As a consequence, the optical functions of a microcrystalline semiconductor can be deduced from its homologue crystalline keeping into account the structural disorder due to the variation of the texture—size, shape, and crystallographic orientation—of crystallites. This distribution of the texture in microcrystalline semiconductors, which we can define as a structural disorder at the medium distance, is indeed the intrinsic feature of microcrystalline materials. This medium structural disorder yields to the potential fluctuations and reduces therefore the coherence length of the photocreated carriers (i.e., the decrease of the lifetime of the photocreated carriers). Interesting conclusions can be deduced from the results of the structural bands calculations by Kramer,[2,3] where the order at the medium distance is relaxed, the electronic conduction bands change in shape accompanied by their ''blurring'' with a negligible effect on the electronic valence bands in many materials (i.e., Si, Ge, and Se).[2,3] We shall give more details for this point in the case of silicon. These results can help us to understand the optical properties of microcrystalline materials and allow us to introduce a supplementary limited lifetime of the excited states and a variation in shape of the structure of the conduction bands. To take into account the effect of the limited crystallite size and the structural medium disorder, the parameters E_p, c_{ij2n}, and Γ_{ij} can be treated as adjustable in Eq. (11). These parameters are characteristic of the medium and are in principle physically significant.

Having found an analytical line shape of the optical dielectric function to simulate the experimental $\varepsilon_2(E)$ spec-

trum for crystalline and microcrystalline semiconductors, it remains only to discuss how to perform the integration in Eq. (11). This integration can be indeed approximated by the rectangular rule. Using this approximation Eq. (11) becomes

$$\varepsilon(E)=\frac{\pi}{2}E_p^2\frac{1}{V_{\mathrm{BZ}}}\sum_i\ \frac{1}{n}\sum_j\ \Delta k_j\sum_l\ \frac{1}{E_{ij1c}(k_{j_1})-E_{ij1v}(k_{j_1})}$$
$$\times\frac{1}{\pi}\frac{\Gamma_{ij}4\pi{k_{j1}}^2}{(E_{ij1c}(k_{j_1})-E_{ij1v}(k_{j_1})-E)^2+(\Gamma_{ij})^2}, \qquad (12)$$

where Δk_j is the increment for sampling the BZ_j and $E_{ijlc(v)}$ is the energy at the k_{jl} point in BZ_j taken from the analytical conduction (valence) bands given in Eq. (11). In Eq. (12) the sum 1 refers to over all k_{jl} points in the BZ_j. Remember that the valence-band state is taken from the crystalline case and should be constant in crystalline and microcrystalline materials.

It is worth noticing that the decrease of the lifetime of the photocreated carriers in microcrystalline materials is also due to the contribution of the recombination process of the photocreated carriers on the deep localized states in the energy gap, due to the dangling bonds in the microcrystalline network. These effects traduce partly in the analytic expression of the imaginary part ε_2 (E) for microcrystalline semiconductors [i.e., Eq. (12)] by adding to the damping effect a broadening, due to the decrease of the lifetime of the photocreated carriers, as $\Gamma(T)=\Gamma_0+\Gamma_\in(T)+\Gamma_{\mathrm{MSD}}+\Gamma_D$, where Γ_{MSD} is the contribution of the medium structural disorder and Γ_D is the contribution of the recombination process of the photocreated carriers on the deep localized states in the energy gap.

As already mentioned above the optical properties of a solid can be described using both the real part and the imaginary part of the complex dielectric function. Such functions are related via Kramers-Kronig dispersion relations [Eq. (1)]. Nevertheless, the use of theses relations requires the knowledge of the ε_1 (E) or the ε_2 (E) spectra in a large spectra range (i.e., high E values) which is not generally the case. In return, the tails of these spectra (i.e., ε_1 or ε_2) can be extended with theoretical functions as the Lorentz or the Drude models depending on the kind of the material.

In order to calculate ε_1 (E) via Kramers-Kronig relations for semiconductor materials, ε_2 (E) can be extended in the high-energy range, with a tail as the Lorentz model. In this classical model only a single transition is considered; ε_2 (E) is given by

$$\varepsilon_2(E)=\frac{A_1CE}{(E^2-E_0^2)^2+C^2E^2}, \qquad (13)$$

where E_0 is the peak transition energy and C is the broadening term. It is worth noticing that the assumption about $\varepsilon_2(E)$ for semiconductor materials in the high-energy range is that which is associated with weakly photocreated carriers.

E. *c*-Si and μc-Si

Let us now discuss the case of *c*-Si and μc-Si materials. It is well known that the imaginary part ε_2 (E) spectrum for *c*-Si in the 1.5–6-eV region can be identified through the direct transitions in both the ΓX and ΓL directions in the BZ. Figure 1 shows such a spectrum; these data are taken from Ref. 8. Three picks are found in the ε_2 (E) spectrum corresponding to (i) the transitions from the highest valence band to the first conduction band in the ΓL direction of the BZ responsible for the peak at 3.4 eV, (ii) the transitions from the highest valence band to both the first and second conduction bands in the ΓX direction of the BZ which is associated with the peak at 4.2 eV, and (iii) the transitions from the highest valence band to the second conduction band in the ΓL direction of the BZ which are associated with the peak at 5.4 eV. Figure 1 also shows the ε_2 (E) spectrum for μc-Si in the 1.5–5-eV range; these data are obtained from Ref. 8. The picks located at 3.4 and 4.2 eV found in the ε_2 (E) spectrum of *c*-Si picks are also observed in the case of microcrystalline silicon, which suggest that the optical properties of this material can be also deduced from both the ΓX and ΓL directions in the BZ. Nevertheless, this spectrum is considerably different in shape from that of *c*-Si. This spectrum is indeed characterized by (i) a marked decrease in the intensity with (ii) greatly weakened 3.4-eV (E_1) and 4.2-eV (E_2) structures, and (iii) a pronounced tail below the *c*-Si fundamental-absorption threshold. Note that the peak located at about 5.4 eV for μc-Si material, while not shown in Fig. 1, is also observed.[17] The observed variations of the optical response between μc-Si and *c*-Si can be explained by the effect of the average crystallite size from the results of the structural band calculations by Kramer[3] on *c*-Si where the order at the medium distance is relaxed by the relation $r_0=a/2\eta$, where r_0 is the distance from where the order is relaxed, a is the crystalline parameter, and η is a constant between 0 and 1. In this work,[3] the electronic properties have been studied within the complex band-structure concept (CBS concept) which

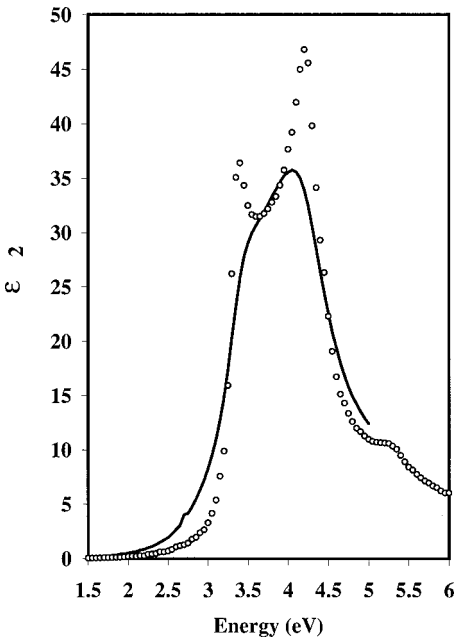

FIG. 1. The imaginary part of the dielectric functions ε_2 for μc-Si (solid curve) and for *c*-Si (open curve) systems. These data are taken from Ref. 8.

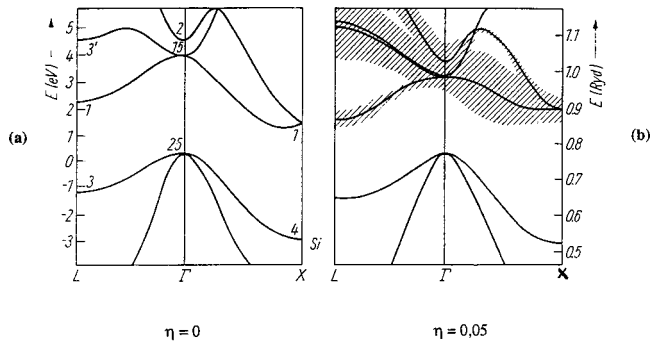

FIG. 2. Complex electronic band structure for Si: (a) infinite crystal ($\eta=0$) and (b) crystal where the order at the medium distance is relaxed ($\eta=0{,}05$). These curves are taken from Ref. 3.

uses the complex energy concept. Figure 2 shows the modification of the electronic band structure when we go from an ideal crystal ($\eta=0$) to a structure where the order at the medium range is relaxed ($\eta=0.05$). This figure shows the change in shape of the electronic conduction bands which are accompanied by a "blurring" (imaginary part of energy), with a negligible effect on the electronic valence band. This blurring, which can be interpreted by the limited lifetime of the excited state, is accompanied by the decrease of the real part of the conduction band energy in the ΓL direction, by the decrease in energy of the direct gap at Γ, and by the increase in the energy gap near *X*. It is worth noticing that the ε_2 (*E*) spectrum for μc-Si shown in Fig. 1 is often called polycrystalline Si (i.e., *p*-Si) with fine grains size. The optical functions of *p*-Si with fine grains can be used to fit in many cases the ellipsometric data of μc-Si layers.[9–10]

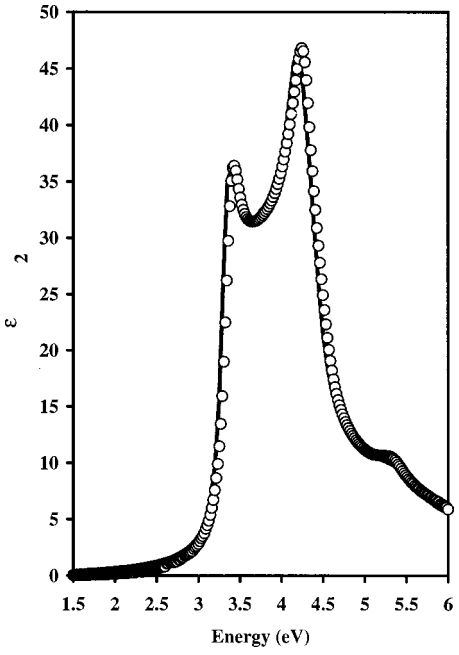

FIG. 3. The imaginary part of the dielectric function ε_2 (open circle) and its best fit (solid curve), obtained with Eq. (12), for *c*-Si. These data are taken from Ref. 8.

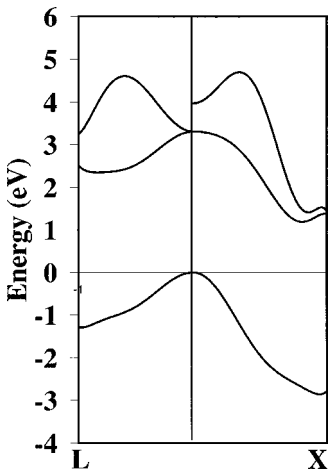

FIG. 4. Electronic band structure for *c*-Si obtained by fitting the experimental dispersion of the ε_2 (*E*) spectrum for *c*-Si with Eq. (12).

III. ANALYSIS AND DISCUSSION

A. *c*-Si

Let us now confront our assumptions to the experimental data. In order to test the consistency of the approximations involved in our phenomenological optical model, we have chosen first the *c*-Si system, where the electronic band structure and the interpretation of its optical response are well known. The dispersion relation (12) could in principle fit the experimental dispersion of ε_2 (*E*) by varying the parameters E_p, c_{ij2n}, and Γ_{ij}. As shown in Fig. 3, perfect agreement between the simulation and the ε_2 (*E*) spectrum has been achieved for *c*-Si using Eq. (12). Interestingly enough the convergence of the parameters with our model has been successfully achieved using the conjugate gradient method.[18] Indeed, the model takes into account the topological considerations, such as the shape and the size of the BZ, which explains the best convergence and less possibility of finding false minima in fitting.

After the excellent agreement between the simulation and the ε_2 (*E*) spectrum, we should discuss whether the parameters of the model are physically significant. The electronic band structure for *c*-Si deduced from the fitted parameters c_{ij2n} is shown in Fig. 4. For more clarity the valence-band structure, obtained by fitting the calculated valence bands for *c*-Si by varying the parameters v_{ij2n} of the analytical equation in Eq. (11), are also shown in this figure. Figure 4 clearly shows that the electronic band structure for *c*-Si obtained with our model is in agreement with those obtained with sophisticated methods. The direct and indirect energy gaps are indeed equal to 3.4 and 1.1 eV, respectively, in excellent agreement with the well-known gaps. The excellent agreement of the conduction bands deduced from the c_{ij2n} parameters with the well-known structure bands corroborates indeed the consistency of the approximations of our model and demonstrates that the parameters c_{ij2n} of the model are physically significant.

Let us now discuss the fitted parameters Γ_{ij}. The values found for these parameters are listed in Table I. This table

TABLE I. The values of the lifetime broadening for each conduction band in ΓL and ΓX directions of the BZ obtained by fitting the experimental dispersion of the $\varepsilon_2(E)$ spectrum for *c*-Si with the Eq. (12).

Γ_{1X} (eV)	Γ_{1L} (eV)	Γ_{2X} (eV)	Γ_{2L} (eV)
0.151	0.067	0.343	0.983

shows that the lifetime broadening increases when we go from the first to the second conduction bands, which explains that the lifetime of the excited states decreases when we go to the second highest conduction bands in the ΓL and ΓX directions of the BZ. The nonzero value of the parameters Γ_{ij} can be easily explained by the interaction between the excited photocreated carriers and the phonons, due to the thermal agitation, and possibly by the interaction between the excited photocreated carriers and the structural defects (i.e., freeze phonons) of the crystalline network.

We now turn to the real part of the dielectric function. As stressed before, the ε_1 (E) spectrum can be deduced from the ε_2 (E) spectrum, in the low-energy range prolonged in the high-energy range with the Lorentz model, via the Kramers-Kronig relation [Eq. (1)]. Figure 5 shows the prolongation of the ε_2 (E) spectrum from 6 to 7 eV with the Lorentz model. The parameters of the Lorentz model in this figure are obtained by fitting the experimental dispersion of ε_2 (E) with the Lorentz formula in the 5.5–6-eV range. The theoretical curve of ε_1 (E) deduced from Fig. 5 up to 15 eV, where the values are close to zero, using the Kramers-Kronig relation could be in principle equal to the experimental dispersion of

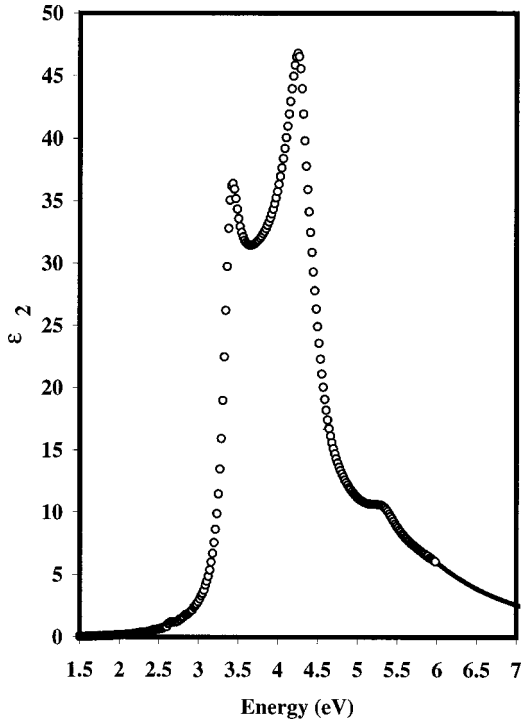

FIG. 5. The imaginary part of the dielectric function ε_2 prolonged with the Lorentz model up to 7 eV for *c*-Si. These data are taken from Ref. 8.

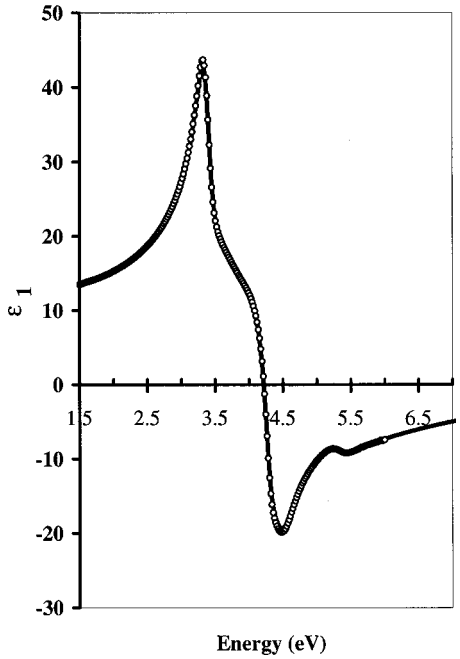

FIG. 6. Experimental spectrum (open circle) and theoretical calculation (solid curve) obtained with the Kramers-Kronig relation of the real part of the dielectric function ε_2 for *c*-Si. These data are taken from Ref. 8.

ε_1 (E). For clarity, we have shown in Fig. 5 only the values up to 7 eV. As shown in Fig. 6, the perfect agreement between the calculation and the experimental dispersion of the ε_1 (E) spectrum, deduced from data of Fig. 5 up to 15 eV, explains that the prolongation of ε_2 (E) is valid.

B. μc-Si

After the success obtained with the example of *c*-Si, in applying the model developed in Sec. II, we have used the same set for μc-Si. As shown in Fig. 7, perfect agreement between the simulation and the ε_2 (E) spectrum has been also achieved for μc-Si using Eq. (12). The band structure for μc-Si deduced from the simulation is shown in Fig. 8; the electronic band structure for *c*-Si of Fig. 4 is also shown for comparison. As expected, according to the discussion in Sec. II E, Fig. 8 shows the modification of the structure of the electronic conduction bands when we go from *c*-Si to μc-Si. The direct band gap decreases indeed with the change in shape of the conduction bands when we go from *c*-Si to μc-Si. This effect can be explained by the decrease of the coherence lengths of the wave functions for the photocreated carriers, due to the medium structural disorder (i.e.,

TABLE II. The values of the lifetime broadening for the first conduction bands in the ΓL and ΓX directions of the BZ obtained by fitting the experimental dispersion of the $\varepsilon_2(E)$ spectrum for μc-Si with Eq. (12).

Γ_{1X} (eV)	Γ_{1L} (eV)
0.203	0.135

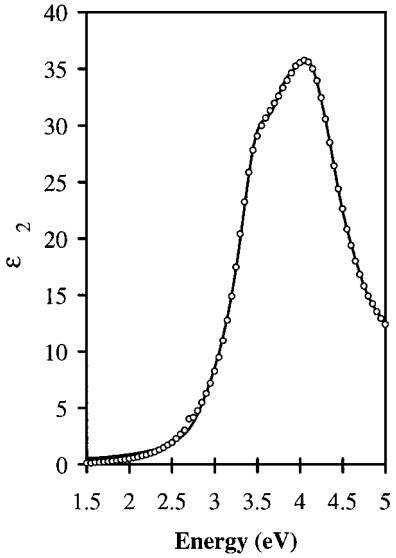

FIG. 7. The imaginary part of the dielectric function ε_2 (open circle) and its best fit (solid curve), obtained with Eq. (12), for μc-Si. These data are taken from Ref. 8.

''random'' distribution of the texture—size, shape, and crystallographic orientation—of crystallites) of the microcrystalline network. Otherwise, this medium structural disorder induces the potential fluctuations in the microcrystalline network and therefore reduces the lifetimes of the photocreated carriers.

Let us now discuss the values found for the fitted parameters Γ_{ij} for μc-Si. These parameters are listed in Table II. The lifetime broadening ratio $(\Gamma_{x1})\mu c$-Si/$(\Gamma_{x1})c$-Si and $(\Gamma_{L1})\mu c$-Si/$(\Gamma_{L1})c$-Si are equal to 1.34 and 2.01, respectively, which suggests that the lifetimes of the photocreated carriers for μc-Si are smaller than for c-Si. These differences can be essentially explained by the effect of the interaction between the excited photocreated carriers and the freeze phonons, due to the medium structural disorder (i.e., random distribution of the texture—size, shape, and crystal-

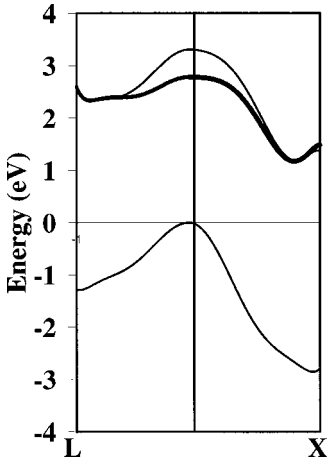

FIG. 8. Electronic band structure for μc-Si obtained by fitting experimental dispersion of ε_2 (E) with Eq. (12); the electronic band structure of Fig. 5 is shown for comparison.

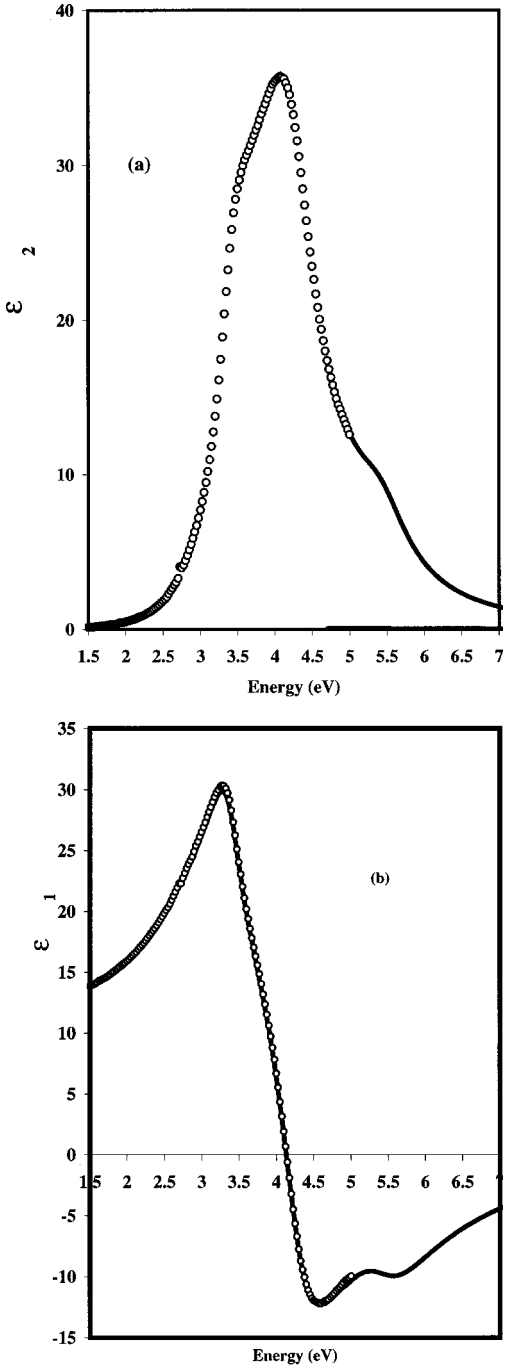

FIG. 9. (a) The imaginary part of the dielectric function ε_2 (open circle) and its best fit (solid curves) and (b) the real part of the dielectric function ε_1 (open circle) and its best fit (solid curves) for μc-Si. The fitting results are obtained by simultaneously fitting the parameters of double absorbing oscillator in the 4.5–5-eV range for ε_2 (E) spectrum and in the 1.5–5-eV range for the ε_1 (E) spectrum, obtained by the Kramers-Kronig transformation.

lographic orientation—of crystallites) of the microcrystalline network. It is important to remember that the ε_2 (E) spectrum for μc-Si has unfortunately measured in a short energy range (i.e., 1.5–5 eV), where we do not have all the information about the transitions from the highest valence band to the second conduction bands in the ΓL and ΓX directions of

the BZ, which contribute on the ε_2 (E) spectrum up to 6 eV. The accuracy of the results of such bands is poorer than that obtained for *c*-Si, where the $\varepsilon_2(E)$ spectrum is measured in the large energy range (i.e., 1.5–6 eV). For this reason, we have not shown the second conduction bands in the ΓL and ΓX directions of the BZ.

As for the calculation for $\varepsilon_1(E)$ for μc-Si material, the theoretical curve deduced from the $\varepsilon_2(E)$ spectrum in the 1.5–5-eV range extended up to 15 eV with a tail from the Lorentz model using the Kramers-Kronig transformation does not agree at all with the experimental dispersion of $\varepsilon_2(E)$. This disagreement can be easily explained by the fact that the $\varepsilon_2(E)$ spectrum, used in the calculation, does not contain the information about the 5.4-eV (E'_1) structure, which is distributed in the full energy range in the $\varepsilon_1(E)$ spectrum. According to the Kramers-Kronig relation, each experimental point of the $\varepsilon_1(E)$ spectrum depends indeed on the whole points of $\varepsilon_2(E)$ in the full energy range. Thus it is obvious that the lack of the information about the 5.4-eV structure in the $\varepsilon_2(E)$ spectrum prolonged with a tail from the Lorentz model yields the disagreement between the experimental data and the calculation of $\varepsilon_1(E)$. Nevertheless, knowing that a part of the information about the 5.4-eV structure in the experimental dispersion of $\varepsilon_2(E)$ is distributed in the 1.5–5-eV range on the $\varepsilon_1(E)$ spectrum, we could in principle via the causality agreement extract therefore this part of the information. Indeed, by combining the prolongation of the experimental dispersion of the $\varepsilon_2(E)$ spectrum with an artificial structure such as a double absorbing oscillator—to take into account the 5.4-eV structure—with the fit of the parameters of this double absorbing oscillator in the 4.5–5-eV range for the $\varepsilon_2(E)$ spectrum and in the 1.5–5-eV range for the $\varepsilon_1(E)$ spectrum, we can on the one hand obtain the best fit of experimental dispersion of $\varepsilon_1(E)$, and on the other hand obtain the information about the 5.4-eV structure in the $\varepsilon_2(E)$ spectrum. As shown in Fig. 9, the satisfactory fitting result has been achieved for the theoretical $\varepsilon_2(E)$ in the 4.5–5-eV range and for the theoretical $\varepsilon_1(E)$ in the 1.5–5-eV range, which explains that the lack of the information about the 5.4-eV structure in the experimental dispersion of $\varepsilon_2(E)$ has been extracted from the experimental dispersion of $\varepsilon_1(E)$ in the 1.5–5-eV range via the causality argument. Note that in this fitting procedure the theoretical curve of $\varepsilon_1(E)$ is deduced from the data of $\varepsilon_2(E)$ up to 15 eV, where the values are close to zero. For clarity, we have shown in Fig. 9 only the values up to 7 eV.

It is worth noticing that our model also allows the parametrization of the optical functions for polycrystalline materials with large grain size. Perfect agreement has been indeed achieved (not shown in this paper) between the optical spectra and the simulation for polycrystalline silicon with large grain size.

As stressed in the introduction, the dispersion formulas are useful to interpret the optical response of thin films. The optical response involves indeed the film parameters such as thickness, dielectric function, and surface roughness. It is common practice to approximate the roughness layer using effective-medium approximation, consisting of 50% voids and 50% of dielectric function.[8–10] Moreover, the measurement of the microcrystalline systems can be influenced by the presence of voids and possibly other mechanisms. The void effect can be approximated by the effective-medium approximation, consisting of a mixture of dense microcrystalline silicon and voids.

IV. CONCLUSION

We have developed a dispersion formula of the optical functions of both crystalline and microcrystalline semiconductors at the energies below and above the lowest gap. This model incorporates the full electronic band structure and the lifetime broadening and its parameters are physically significant. With the example of crystalline silicon, we have demonstrated the good agreement between the simulation and optical spectra (i.e., dielectric function). It is shown that the electronic band structure for *c*-Si obtained from the fitted parameters is in agreement with the well-known electronic band structure, which demonstrates the consistency of the approximation of the model. After the success obtained with the example of *c*-Si, we have used the same set for μc-Si. It is shown that the general change in the optical functions in microcrystalline silicon materials compared to their homologue crystalline materials is due to the effects of the decrease of the coherence lengths of the wave functions for the photocreated carriers, due to the medium structural disorder (i.e., random distribution of the texture—size, shape, and crystallographic orientation—of crystallites), which yields to the change in shape of the electronic conduction bands and the decrease of the lifetime of the excited states.

ACKNOWLEDGMENTS

The authors wish to thank Dr. B. Drevillon, Dr. R. Benferhat, and Dr. M. Stchakovsky, for their interest in this work.

*Present address: Jobin-Yvon Thin Films Group, Z.A. La Vigne aux Loups 7, Avenue Arago 91 380 Chilly Mazarin, France; email address: htouir@jyhoriba.fr

[1] F. Bassani and G. Pastori Parravicini, in *Electronic States and Optical Transitions*, edited by R. A. Ballinger (Pergamon, Oxford, 1975), pp. 67–103.

[2] B. Kramer, Phys. Status Solidi **41**, 649 (1970).

[3] B. Kramer, Phys. Status Solidi B **47**, 501 (1971).

[4] Y. Mishima, S. Miyazaki, M. Hirose, and Y. Osaka, Philos. Mag. B **46**, 1 (1982).

[5] F. Siebke, S. Yata, Y. Hishikawa, and M. Tanaka, J. Non-Cryst. Solids **227**, 9777 (1998).

[6] N. Bech, J. Meier, J. Fric, Z. Remmes, A. Poruba, R. Fluckiger, J. Pohl, A. Shah, and M. Vanecek, J. Non-Cryst. Solids **198&200**, 903 (1985).

[7] H. Touir, Ph.D. thesis, Université Pierre et Marie Curie de Paris,

France, 1997.
[8] G. E. Jellison, M. F. Chisholm, and S. M. Gorbakin, Appl. Phys. Lett. **62**, 3348 (1993).
[9] S. Hamma, Ph.D. thesis, Université Pierre et Marie Curie de Paris, France, 1998.
[10] S. Hamma and P. Roca i Cabarrocas, Sol. Energy Mater. Sol. Cells **69**, 217 (2001).
[11] A. F. Fourouhi and I. Bloomer, in *Handbook of Optical Constants of Solids II*, edited by Edward D. Palik (Academic, Boston, 1991), pp. 151–175.
[12] Sadao Adachi, Phys. Rev. B **35**, 7454 (1987).
[13] Toshiaki and Sadao Adachi, J. Appl. Phys. **69**, 1574 (1991).
[14] Charles C. Kim, J. W. Garland, H. Abad, and P. M. Raccah, Phys. Rev. B **45**, 11 749 (1991).
[15] F. Bassani and G. Pastori Parravicini, in *Electronic States and Optical Transitions*, edited by R. A. Ballinger (Pergamon, Oxford, 1975), pp. 149–176.
[16] S. Albrecht and L. Reining, Phys. Rev. Lett. **80**, 4510 (1998).
[17] B. G. Bagley, D. E. Aspnes, A. C. Adams, and C. J. Mogab, Appl. Phys. Lett. **38**, 56 (1981).
[18] William H. Press, Brian P. Flannery, Saul A. Tenkolsky, and William T. Vetterlin, in *Numerical Recipes in Pascal*, (Cambridge University Press, Cambridge, UK, 1989), pp. 339–345.